Multi-objective Bayesian global optimization for continuous problems and applications

Yang, K.

Chapter 4

TEHVI Calculation[1]

In optimization with expensive black box evaluations, the expected improvement algorithm (also called *efficient global optimization*) is a commonly applied method. It uses Gaussian Processes (or Kriging) to build a model of the objective function and uses the expected improvement as an infill criterion, taking into account both – predictive mean and variance. EI has been generalized to multi-objective optimization using the expected hypervolume improvement, which measures the expected gain in the hypervolume indicator of a Pareto front approximation, as shown in Chapter 3. However, this criterion assumes an unbounded objective space even if it is often known a-priori that the objective function values are within a prescribed range, e.g., lower bounded by zero. Taking advantage of such a-priori knowledge, this chapter introduces the truncated expected hypervolume improvement and a multi-objective efficient global optimization method that is based on TEHVI. This chapter shows how to compute the truncated expected hypervolume improvement exactly and efficiently. Then it is tested as an infill criterion in efficient global optimization. It is shown that it can effectively make use of a-priori knowledge and achieve better results in cases where such knowledge is given. The usefulness of the new approach is demonstrated on benchmark examples. The empirical studies in this chapter are confined to the bi-objective case.

This chapter is structured as follows: Section 4.1 introduces the motivations of the TEHVI research; Section 4.2 provides the definition of TEHVI and the formula to calculate exact TEHVI, including asymptotic complexity analysis and CPU time assessment; Sections 4.3 and 4.4 show the experimental settings and empirical

[1]This chapter only considers minimization problems.

experimental results, respectively.

4.1 Motivations

Many algorithms exist in the multi-objective optimization field. For the evolutionary algorithm class, NSGA-II [75] and SMS-EMOA [19] are two well-known algorithms. Surrogate-model based optimization strategies, which replace exact evaluations by approximations learned from past evaluations, are another important branch. Compared to evolutionary algorithms, surrogate-model based algorithms need a small budget of function evaluations. Because of this, they are often used in the real world design optimization with expensive evaluations.

A simple and common sequential optimization scheme is to sequentially update the surrogate model by evaluations the points that are promising due to the prediction. The prospects of a new point are assessed by the so-called infill criterion. In the context of Gaussian process models, the expected improvement criterion is a commonly applied infill criterion. It takes into account both the predictive mean and the predictive variance of the surrogate model. Therefore it promotes evaluations in less explored regions that have a higher predictive variance. In single-objective optimization the expected improvement was introduced in 1978 by Mockus et al. [37], and became more popular due to the work of Jones et al. [41]. It was generalized to the expected hypervolume improvement (EHVI) for multi-objective optimization by Emmerich [56].

There are alternative generalizations of the expected improvement in the filed of multi-objective optimization. Among them, EHVI has a good convergence to a diverse approximation of the Pareto front, however, exact calculation of EHVI used to be time-consuming [69]. Recently, new algorithms for computing EHVI in the bi-objective EHVI-EGO have been found. Hupkens et al. improved the time complexity to $O(n^2)$ [1]. More recently, Emmerich et al. devised an asymptotically optimal algorithm with time complexity $O(n \log n)$ [2] in the bi-objective case, where n is the number of non-dominated points in the archive. This makes EHVI-EGO competitive with other techniques that use fast computable infill criteria, in particular SMS-EGO.

Besides its time consumption, EHVI does not take into account some known domain information of the objective function. Expected hypervolume improvement (EHVI) is the expected increment of the hypervolume indicator, which is related to the current approximation of the Pareto front and a predictive multivariate

Gaussian distribution of a new point [10]. That is to say, EHVI is based on the assumption that the objective values follow a normal distribution, and prediction of the objective values are from minus infinity to plus infinity. However, in some cases, we already know an approximation range of the objective value. For instance, in a PID parameter tuning problem, the rising time is always a positive value. In this case, we assumed surrogate-model based algorithms could converge to true Pareto front faster, if the multivariate Gaussian distribution in EHVI is truncated to the objective function's co-domain.

For using the co-domain information, this chapter introduces the truncated expected hypervolume improvement (TEHVI) based on EHVI. TEHVI is based on the normal distribution, which is truncated by the objective value domain. In terms of Bayesian reasoning, it uses the conditional distribution given the a-priori knowledge. This knowledge is about the true output of the objective function within a prescribed range. Practically speaking, the idea behind TEHVI is to focus sampling on more relevant parts of the search space by taking into account a-priori knowledge on objective function value ranges. It is hypothesized that this will speed up the convergence of the Pareto front.

This section mainly discusses the formula to calculate truncated expected hypervolume improvement. It will also have asymptotically optimal time $\Theta(n \log n)$, and empirical validation and speed comparison between Monte Carlo method and the TEHVI exact method.

4.2 TEHVI Definition

Definition 4.1 (Truncated Expected Hypervolume Improvement) [2] *Given parameters of the multivariate predictive distribution $\boldsymbol{\mu}$, $\boldsymbol{\sigma}$ and the Pareto-front approximation $\mathbf{P}$, a preferred multidimensional range $[\mathbf{A}, \mathbf{B}] = [A_1, B_1] \times \cdots [A_d, B_d] \subset \mathbb{R}^d$ in the objective space. Suppose an objective value vector $\mathbf{y}$ follows the truncated normal distribution and lies within an interval $\mathbf{y} \in (\mathbf{A}, \mathbf{B})$, where $-\boldsymbol{\infty} \leq \mathbf{A} < \mathbf{B} \leq \boldsymbol{\infty}$, then the truncated expected hypervolume improvement (TEHVI) is defined as:*

$$TEHVI(\boldsymbol{\mu}, \boldsymbol{\sigma}, \mathbf{P}, \mathbf{r}, \mathbf{A}, \mathbf{B}) := \int_{\mathbf{y} \in [\mathbf{A}, \mathbf{B}]} HVI(\mathbf{P}, \mathbf{y}) \cdot TPDF_{\boldsymbol{\mu}, \boldsymbol{\sigma}}(\mathbf{y}) d\mathbf{y} \qquad (2\text{-}1)$$

[2] The prediction of $\boldsymbol{\mu}$ and $\boldsymbol{\sigma}$ depends on a Kriging model and a target point $\mathbf{x}$ in the search space. Explicitly, TEHVI is dependent on the target point $\mathbf{x}$.

where $TPDF_{\boldsymbol{\mu},\boldsymbol{\sigma}}$ *is the truncated multivariate independent normal distribution with mean values* $\boldsymbol{\mu} \in \mathbb{R}^d$ *and standard deviations* $\boldsymbol{\sigma} \in \mathbb{R}^d_+$.

Here, $TPDF_{\boldsymbol{\mu},\boldsymbol{\sigma}}$ is the probability density function for the event that $\mathbf{y}$ is the result of the function evaluation, given function evaluations that are not within the range $[\mathbf{A}, \mathbf{B}]$ would be rejected. Due to rejection of values outside the range, in Bayesian reasoning we could use the information $\mathbf{y} \in [\mathbf{A}, \mathbf{B}]$ (after acceptance) as a Bayesian prior.

Example 4.1 *An illustration of the EHVI is shown in Figure 4.1. The light gray area is the dominated subspace of* $\mathbf{P} = \{\mathbf{y}^{(1)} = (3,1)^\top, \mathbf{y}^{(2)} = (2,1.5)^\top, \mathbf{y}^{(3)} = (1,2.5)^\top\}$ *cut by the reference point* $\mathbf{r} = (0,0)^\top$. *The bivariate Gaussian distribution has the parameters* $\mu_1 = 2$, $\mu_2 = 1.5$, $\sigma_1 = 0.7$, $\sigma_2 = 0.6$. *The truncated probability density function (TPDF) of the bivariate Gaussian distribution is indicated as a 3-D plot, with truncated domains* $[\mathbf{A}, \mathbf{B}] = [\mathbf{1}, \boldsymbol{\infty}]$. *Here* $\mathbf{y}$ *is a sample from this distribution and the area of improvement relative to* $\mathbf{P}$ *is indicated by the dark shaded area. The variable* y_1 *stands for the* f_1 *value and* y_2 *for the* f_2 *value.*

4.2.1 Formula Derivation

For the aim of calculating the truncated expected hypervolume improvement, we need to define the truncated PDF (ϕ_T) and truncated CDF (Ψ_T) functions first. Suppose the co-domain of a truncated normal distribution is [A, B], where $-\infty \leq A < B \leq \infty$. From the definition of truncated normal distribution, ϕ_T and Φ_T functions are defined as follows[76]:

$$\phi_T(x) = \begin{cases} 0 & \text{if } x \leq A \text{ or } x \geq B \\ \mathbf{Z}(A,B) \cdot \frac{\phi(\frac{x-\mu}{\sigma})}{\sigma} & \text{if } A < x < B \end{cases} \tag{2-2}$$

$$\Phi_T(x) = \begin{cases} 0 & \text{if } x \leq A \\ \mathbf{Z}(A,B) \cdot [\Phi(\frac{x-\mu}{\sigma}) - \Phi(\frac{A-\mu}{\sigma})] & \text{if } A < x < B \\ 1 & \text{if } x \geq B \end{cases} \tag{2-3}$$

$$\text{where: } \mathbf{Z}(A,B) = 1/[\Phi(\frac{B-\mu}{\sigma}) - \Phi(\frac{A-\mu}{\sigma})] \tag{2-4}$$

Due to the independence of the multivariate Gaussian distributions for each objective, the product of the truncated distributions can be computed using Fubini's

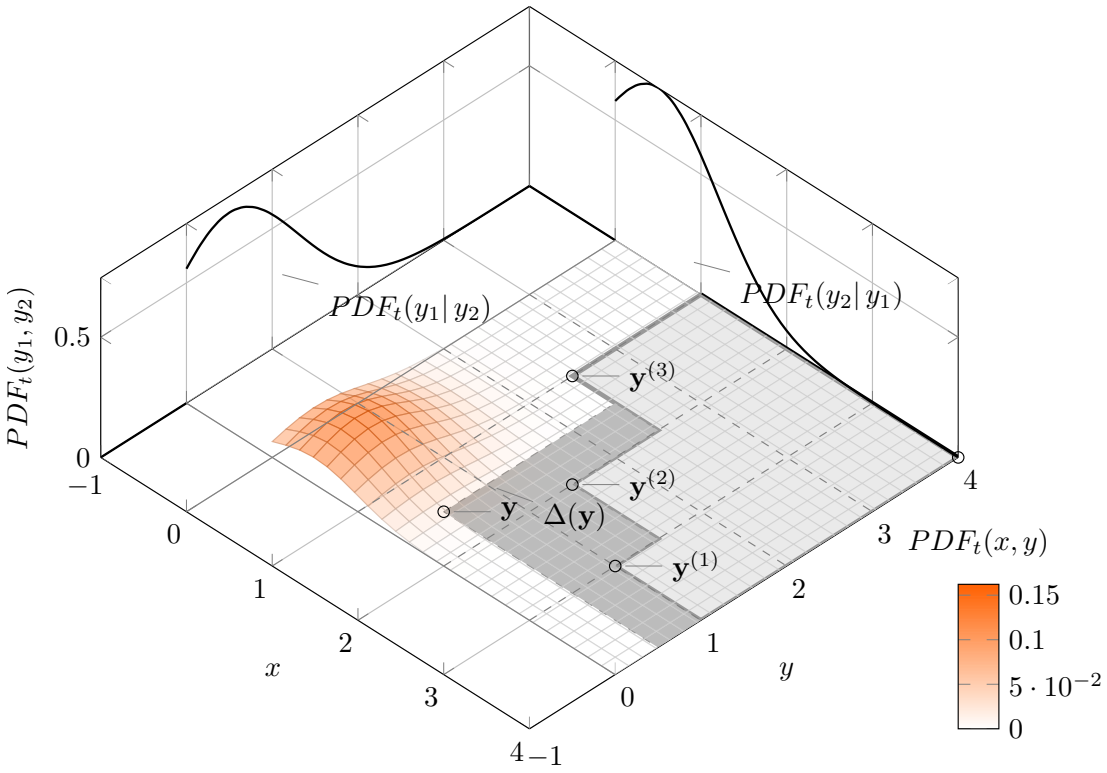

Figure 4.1: TEHVI in 2-D (cf. Example 4.1).

law. What needs to be done is to replace Φ by Φ_T and Ψ by Ψ_T in the original computation, with interval boundaries chosen according to the interval boundaries. Based on $\Theta(n \log n)$ 2-D EHVI formula (minimization case) in A.4, the TEHVI formula can be written as:

$$
\begin{aligned}
&\mathrm{TEHVI}(\boldsymbol{\mu}, \boldsymbol{\sigma}, \mathrm{Y}, \mathbf{r}, A, B) \\
&= \int_{y_1=-\infty}^{\infty} \int_{y_2=-\infty}^{\infty} \sum_{i=1}^{n+1} \lambda_2[S_i \cap \Delta(y_1, y_2)] \cdot PDF_{\boldsymbol{\mu},\boldsymbol{\sigma}}(\mathbf{y}) d\mathbf{y} \\
&= \sum_{i=1}^{n+1} (y_1^{(i-1)} - y_1^{(i)}) \cdot \Phi_T \left(\frac{y_1^{(i)} - \mu_1}{\sigma_1} \right) \cdot \Psi_T(y_2^{(i)}, y_2^{(i)}, \mu_2, \sigma_2) + \\
&\quad \sum_{i=1}^{n+1} \left(\Psi_T(y_1^{(i-1)}, y_1^{(i-1)}, \mu_1, \sigma_1) - \Psi_T(y_1^{(i-1)}, y_1^{(i)}, \mu_1, \sigma_1) \right) \times \\
&\qquad \Psi_T(y_2^{(i)}, y_2^{(i)}, \mu_2, \sigma_2)
\end{aligned}
\tag{2-5}
$$

According to the definition of truncated normal distribution and the formula of

normal *exipsi* function (Ψ), the truncated *exipsi* function (Ψ_T) for minimization problems can be derived by the following procedure:

$$\begin{aligned}\Psi_T(a,b,\mu,\sigma,A,B)_{min} &= \int_A^b (a-z)\frac{1}{\sigma}\phi_T(\frac{z-\mu}{\sigma})dz \\ &= \int_A^b (a-z)\cdot \mathbf{Z}(A,B)\cdot\frac{1}{\sigma}\phi(\frac{z-\mu}{\sigma})dz \\ &= \mathbf{Z}(A,B)\cdot\int_A^b (a-z)\frac{1}{\sigma}\phi(\frac{z-\mu}{\sigma})dz \\ &= \mathbf{Z}(A,B)\cdot[(\sigma\phi(\frac{b-\mu}{\sigma})+(a-\mu)\Phi(\frac{b-\mu}{\sigma})- \\ &\qquad (\sigma\phi(\frac{A-\mu}{\sigma})+(a-\mu)\Phi(\frac{A-\mu}{\sigma}))] \end{aligned} \tag{2-6}$$

In some cases, it is difficult to transform maximization problems to minimization problems. For solving it, the truncated *exipsi* function for maximization problems is necessary and it is:

$$\begin{aligned}\Psi_T(a,b,\mu,\sigma,A,B)_{max} &= \int_b^B (a-z)\frac{1}{\sigma}\phi_T(\frac{z-\mu}{\sigma})dz \\ &= \mathbf{Z}(A,B)\cdot[(\sigma\phi(\frac{b-\mu}{\sigma})+(\mu-a)(1-\Phi(\frac{b-\mu}{\sigma}))- \\ &\qquad (\sigma\phi(\frac{B-\mu}{\sigma})+(\mu-a)(1-\Phi(\frac{B-\mu}{\sigma}))] \end{aligned} \tag{2-7}$$

4.2.2 Computational Speed Test

In this subsection the computational speed of TEHVI computation is assessed when there are different population sizes. For validation purposes, the results are compared with results from Monte Carlo integration. The acceptance-rejection method [77] was used as the sampling strategy in Monte Carlo method. Samples out of the feasible interval range were rejected. The Monte Carlo method was allowed to run for 100,000 iterations. All the experiments were performed on the same computer: Intel(R) i7-3770 CPU @ 3.40GHz, RAM 16GB. The operating system was Ubuntu 14.04 LTS (64 bit), complier was gcc 4.9.2 with flag '-Ofast' for exact method, and platform was MATLAB 8.4.0.150421 (R2014b), 64 bit for Monte Carlo method.

Fig 4.2, the left subfigure is the randomly generated Pareto fronts with the type of convexSpherical and concaveSpherical in the 2-D case from [20]. The

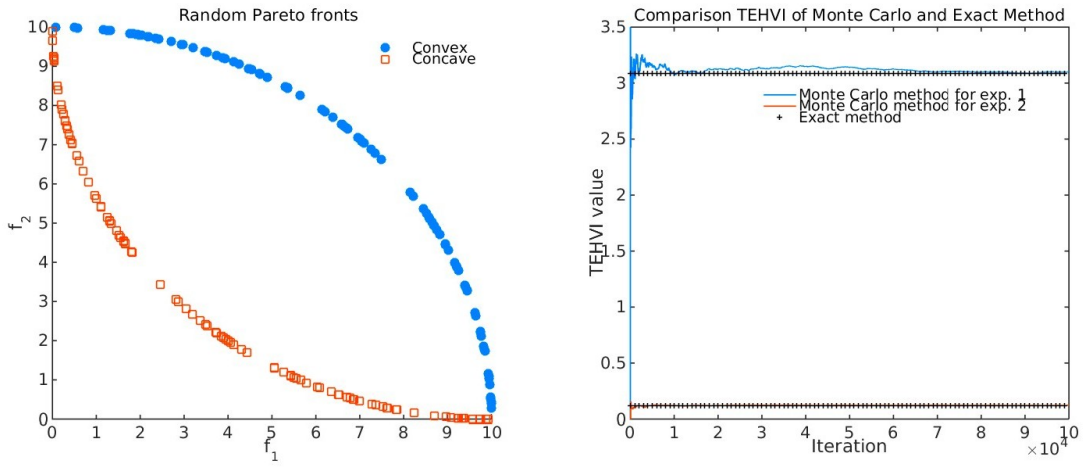

Figure 4.2: Left: Randomly generated fronts with $|P| = 100$. Right: TEHVI comparison of Monte Carlo method and exact method.

right subfigure shows the convergence of Monte Carlo integration to the Pareto fronts. The evaluated points are (9.9955, 0.3001) and (8.4149, 0.1264) for experiment 1 (convex Pareto front) and experiment 2 (concave Pareto front), respectively. The reference point for both experiments was (15,15). It shows that the TEHVI value based on Monte Carlo method is similar to exact method after 50,000 iterations. However, the Monte Carlo method needs more iterations to generate a sufficiently accurate TEHVI value.

Table 4.1 shows the empirical speed experiments between exact TEHVI calculation method and Monte Carlo method. The parameters: $\sigma_m = 2.5$, $\mu_m = 10$ and $m = 2$ were used to randomly generate Pareto fronts in the experiments. Pareto front sizes $|P| \in \{10, 100, 1000\}$ and different number of predictions (candidate points) of Batch Size are used together with σ_m and μ_m. In the experiments, *batch mode* means that the Pareto front population does not change and computations of transcendental functions (erf, exp) on grid coordinates can be re-used. This results in a significant speed-up in the empirical performance, although the time complexity is not affected. 10 trials were randomly generated by the same parameters, and average runtimes (10 runs) for the whole trails with the same parameters were computed. It shows that the exact and efficient TEHVI calculation method is fast, even for large population sizes of 1000 points it can be computed in ca. 1 second. It is also fast when compared to an imprecise Monte Carlo method. Note that this study should not be used as a speed comparison, as the Monte Carlo method is not precise. However, it indeed shows that the time consumption of the Monte Carlo method increases quickly.

Table 4.1: TEHVI computation speed experiments results.

Type	$\|P\|$	Batch Size	Time_average (s)	
			Exact	Monte Carlo
CONVEX	10	1	0.00005	3.82615
CONVEX	10	10	0.00019	37.56125
CONVEX	10	100	0.00166	379.19625
CONVEX	10	1000	0.02030	> 10 min
CONVEX	100	1	0.00022	13.34105
CONVEX	100	10	0.00165	140.10564
CONVEX	100	100	0.01654	> 10 min
CONVEX	100	1000	0.16084	> 10 min
CONVEX	1000	1	0.00208	203.11692
CONVEX	1000	10	0.01644	> 10 min
CONVEX	1000	100	0.16746	> 10 min
CONVEX	1000	1000	1.69174	> 10 min
CONCAVE	10	1	0.00006	3.89077
CONCAVE	10	10	0.00016	39.15924
CONCAVE	10	100	0.00142	389.16426
CONCAVE	10	1000	0.01585	> 10 min
CONCAVE	100	1	0.00023	13.95431
CONCAVE	100	10	0.00150	138.14462
CONCAVE	100	100	0.01457	> 10 min
CONCAVE	100	1000	0.14779	> 10 min
CONCAVE	1000	1	0.00203	204.58791
CONCAVE	1000	10	0.01494	> 10 min
CONCAVE	1000	100	0.14657	> 10 min
CONCAVE	1000	1000	1.53391	> 10 min

4.3 Experimental Setup

In the comparison, nine test problems are used. They are: BK1 [78], SSFYY1 [79], ZDT1, ZDT2, ZDT3, ZDT4, ZDT6[80], generalized Schaffer problem (GSP) [81] and PID parameter tuning problem.

The parameters for the algorithms are shown in Table 4.2.

Table 4.2: Parameter settings.

Algorithm	μ/Initial Population	λ	iteration	p_c	p_m
EHVI-EGO	30	/	200	/	/
TEHVI-EGO	30	/	200	/	/
NSGA-II	30	30	200	0.9	1/N
SMS-EMOA	30	/	200	0.9	1/N

The TEHVI-EGO boundary (A, B) for all the experiments are $(0, \infty)$, except for the ZDT3 problem. Since the lower bound of ZDT3 is close to -1, the TEHVI-EGO boundary for ZDT3 was set to $(-1, \infty)$. For the generalized Schaffer problem, the parameter γ was set as $\gamma = 0.4$. All the experiments were repeated 5 times.

4.4 Empirical Results

Table 4.3 shows the results for all the test problems. TEHVI-EGO and EHVI-EGO are better than the other two algorithms. Among the EGO based algorithms, TEHVI-EGO performs slightly better than EHVI-EGO. The reason for these results is that all the fitness values for all the problems are positive, except for the ZDT3, and the truncation forces the optimization algorithm to focus on the fitness spaces in the positive domain. Figure 4.3 shows the Pareto fronts generated by 4 different algorithms for generalized Schaffer problem (GSP) in the left. The Pareto fronts generated by TEHVI-EGO and EHVI-EGO are much closer to true Pareto front than the other two algorithms. Compared to the performance of EHVI-EGO with respect to HV, HV of TEHVI-EGO Pareto front is slightly bigger than that of EHVI-EGO. The interval boundaries for TEHVI-EGO are set to $A = 0, B = \infty$ in Figure 4.3 (right). This is based on the assumption that only the lower bound of the fitness value is known.

However, the strategy for setting the interval boundary is tricky. In Figure 4.3, the right plot shows the Pareto fronts generated by TEHVI-EGO with different interval boundary. In this case, the (red) squared Pareto front focuses on the knee points with more points but can not explore the extreme boundary of the true Pareto front well, when compared to the (blue) triangle one. Meanwhile,

Table 4.3: Empirical comparison of different algorithms for test problems.

Test Function	Methods	reference point	Pareto front size				HV			
			max	min	mean	std	max	min	mean	std
BK1	EHVI-EGO	[60 60]	126	118	121.6	3.5071	3176.3411	3175.8606	3176.0758	0.2057
BK1	TEHVI-EGO	[60 60]	131	120	**124.6**	4.6690	**3176.4359**	3175.8961	**3176.1843**	0.2451
BK1	NSGA-II	[60 60]	58	53	55.6	2.0736	3132.1585	3126.3921	3129.2289	2.3525
BK1	SMS-EMOA	[60 60]	51	50	50.8	0.4472	3035.8162	2889.2727	2964.0079	65.9014
SSFYY1	EHVI-EGO	[5 5]	99	91	93.8	3.1145	20.7376	20.7308	20.7345	0.0027
SSFYY1	TEHVI-EGO	[5 5]	100	88	**95**	5.0990	**20.7431**	20.7269	**20.7355**	0.0062
SSFYY1	NSGA-II	[5 5]	57	53	55.6	1.6733	20.3667	20.1943	20.2895	0.0662
SSFYY1	SMS-EMOA	[5 5]	51	43	47.4	4.0373	18.5052	16.2884	17.6106	0.8399
ZDT1	EHVI-EGO	[15 15]	64	43	**56.2**	8.0436	224.6547	224.6409	224.6468	0.0064
ZDT1	TEHVI-EGO	[15 15]	71	40	52.6	11.4149	**224.6569**	224.6461	**224.6502**	0.0044
ZDT1	NSGA-II	[15 15]	45	39	43.2	2.4900	224.6172	220.7671	222.7442	1.7513
ZDT1	SMS-EMOA	[15 15]	51	48	49.4	1.1402	218.6193	217.7475	218.2609	0.3504
ZDT2	EHVI-EGO	[15 15]	27	24	26	1.2247	224.3152	224.2933	224.3099	0.0093
ZDT2	TEHVI-EGO	[15 15]	29	27	28.2	1.0954	**224.3168**	224.3151	**224.3161**	0.0008
ZDT2	NSGA-II	[15 15]	57	44	**47.8**	5.4037	224.0502	210.1391	213.4889	5.9302
ZDT2	SMS-EMOA	[15 15]	22	10	16	5.6569	189.7940	176.3485	184.7327	6.0880
ZDT3	EHVI-EGO	[15 15]	20	12	17.8	3.4928	235.8485	235.8015	235.8328	0.0196
ZDT3	TEHVI-EGO	[15 15]	32	15	21	6.8191	**235.8495**	235.8039	**235.8359**	0.0183
ZDT3	NSGA-II	[15 15]	47	42	**44.2**	1.9235	235.7032	221.2648	228.3704	5.3756
ZDT3	SMS-EMOA	[15 15]	31	16	24	5.7879	207.4997	202.1116	204.0837	2.1858
ZDT4	EHVI-EGO	[15 15]	7	3	4.4	1.6733	224.3295	204.4661	217.2593	8.0295
ZDT4	TEHVI-EGO	[15 15]	11	6	7.4	2.0736	**224.5959**	217.9858	**221.3740**	2.9304
ZDT4	NSGA-II	[15 15]	47	37	**43.2**	4.1473	215.6850	184.2184	203.9832	12.6032
ZDT4	SMS-EMOA	[15 15]	20	5	13	5.3385	145.3309	116.0149	127.4335	36.2023
ZDT6	EHVI-EGO	[15 15]	25	16	19.6	3.7815	218.7974	218.7442	218.7843	0.0228
ZDT6	TEHVI-EGO	[15 15]	32	19	23.3	6.1305	**218.8301**	218.7871	**218.8095**	0.0178
ZDT6	NSGA-II	[15 15]	41	25	**35.2**	7.2938	218.6877	155.9356	198.5166	26.2609
ZDT6	SMS-EMOA	[15 15]	22	7	11.6	6.0249	145.3309	116.0149	127.4335	11.8642
GSP	EHVI-EGO	[5 5]	167	140	161.4	11.9708	24.9066	24.9063	24.9065	0.0001
GSP	TEHVI-EGO	[5 5]	169	154	**166**	6.7082	**24.9066**	24.9066	**24.9066**	<0.0001
GSP	NSGA-II	[5 5]	60	56	58	2.0000	24.8933	24.8838	24.8903	0.0040
GSP	SMS-EMOA	[5 5]	51	50	50.8	0.4472	24.8605	24.6154	24.7519	0.1140

the HV value of the red squared Pareto front is smaller than blue triangle one. The reason for the difference is that the precise integration domain $(0, 1)$ is much smaller than $(0, \infty)$. This could lead to the low probability of exploration at the extreme boundary, which is close to infinity, and high probability of sampling the area on the Pareto front, which is closer to the minimization point (in this case, this point is $(0, 0)$).

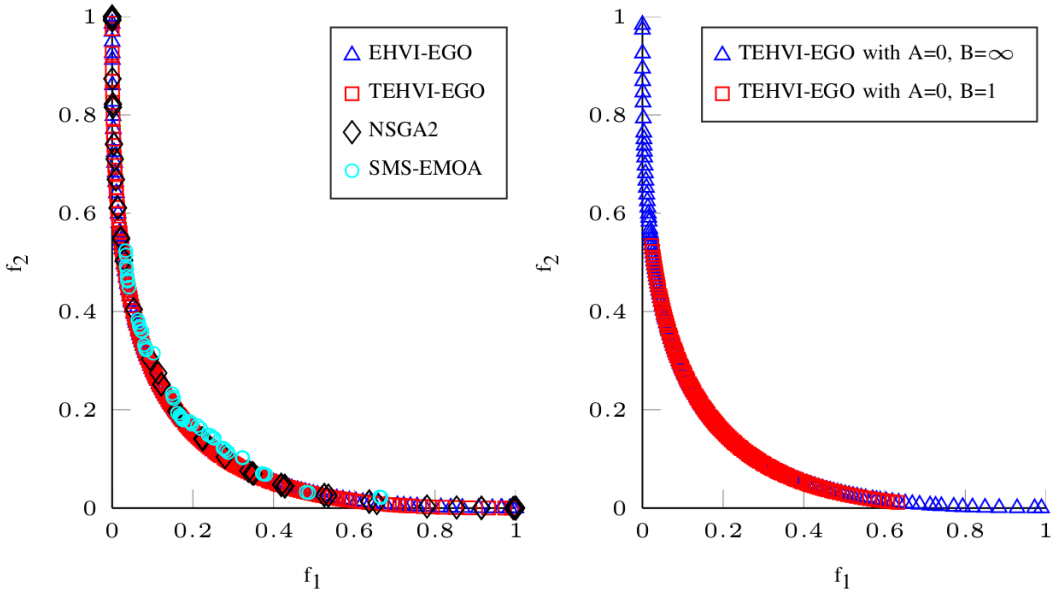

Figure 4.3: Left: The results of one trial experiment for GSP in Table 4.3. Right: TEHVI-EGO with different interval boundary.

4.5 Summary

In this chapter, we introduced an exact method for the calculation of the truncated expected hypervolume improvement and investigated different multi-objective optimization algorithms for the benchmarks and the optimization of a controller. In particular, the two state-of-the-art evolutionary algorithms (NSGA-II and SMS-EMOA) were compared with multi-objective efficient global optimization algorithms (EHVI-EGO and TEHVI-EGO), which utilize a surrogate model of the objective function. Among the 9 test problems, TEHVI-EGO yielded better results than the other three algorithms, with respect to HV.

As the TEHVI only calculates the EHVI in a particular domain, and can force the algorithm on exploring in this domain, TEHVI-EGO exhibits poor performance of exploring the extreme boundaries for the Pareto fronts, when the interval codomain is set as the boundary of the fitness. However, in this case, TEHVI-EGO, compared to EHVI-EGO, can focus on the knee point of the Pareto fronts, which could be used when a particular domain of a Pareto front is attractive.

To summarize, based on the result of this study, we recommend using TEHVI-EGO when boundaries of domain regions are known, because it shows a good performance more consistently when compared to the other algorithms. In addition, it can focus on the Pareto front in a particular domain. For the further work, it is recommended to research the gradient of TEHVI.